SLAC – PUB – 4334
May 1987
(T/E)

Searching for 4th Generation Fermions at High–Energy e^+e^- Machines*

JONATHAN DORFAN AND RICHARD J. VAN KOOTEN
Stanford Linear Accelerator Center
Stanford University, Stanford, California 94305

1. Introduction

This writeup summarizes Monte Carlo studies on the feasibility of searching for 4th family fermions at high energy e^+e^- machines. By high energy we mean energies beyond the Z°; the Z° searches having been studied extensively by the SLC and LEP collaborations. We have chosen the specific examples of $\sqrt{s} =$ 200 GeV (namely LEP200) and $\sqrt{s} = 600$ GeV (in line with work being done at SLAC to investigate the potential of a future linear collider). The studies have been performed with the four vectors produced by the models and no attempt has been made to account for the effects of finite resolution and inefficiencies due to a real detector environment.

We will begin by considering a canonical 4th family in the Standard Model:

$$\begin{pmatrix} u \\ d \end{pmatrix} \quad \begin{pmatrix} c \\ s \end{pmatrix} \quad \begin{pmatrix} t \\ b \end{pmatrix} \quad \begin{pmatrix} h \\ \ell \end{pmatrix}$$

$$\begin{pmatrix} e^\pm \\ \nu_e \end{pmatrix} \quad \begin{pmatrix} \mu^\pm \\ \nu_\mu \end{pmatrix} \quad \begin{pmatrix} \tau^\pm \\ \nu_\tau \end{pmatrix} \quad \begin{pmatrix} L^\pm \\ \nu_L \end{pmatrix}$$

and will return later to the possibility that the 4th generation neutral lepton is in fact massive.

* Work supported by the Department of Energy, contract DE–AC03–76SF00515.

Presented at the First International Symposium on the 4th Family of Quarks and Leptons, Santa Monica, California, February 26–28, 1987.

2. Production, Decay and Backgrounds

The attractiveness of the e^+e^- environment is the direct and relatively background-free production of the fundamental fermions; in all cases studied here the 4th family fermions $(f, \bar{f})$ are produced in pairs via the intermediate exchange of a virtual photon or Z°. The production cross section for this process $e^+e^- \to \gamma$, $Z^\circ \to f\bar{f}$ is given by the Electroweak Model:

$$\frac{d\sigma}{d\cos\theta} = \frac{3\pi\alpha^2 Q_f^2}{2s}(1+\cos^2\theta)$$
$$- \frac{\alpha D G_F Q_f M_z^2(s-M_z^2)}{8\sqrt{2}[(s-M_z^2)^2+\Gamma_z^2 M_z^2]} \cdot [4v_e v_f(1+\cos^2\theta)+8a_e a_f\cos\theta]$$
$$+ \frac{D G_F^2 M_z^4 s}{64\pi[(s-M_z^2)^2+\Gamma_z^2 M_z^2]} \cdot [4(a_e^2+v_e^2)(a_f^2+v_f^2)+32a_e v_e a_f v_f\cos\theta]$$

where θ is the production angle of the fermion, a and v are the weak couplings, s is the center-of-mass energy squared, M_z and Γ_z are the mass and width of the Z°, Q_f the fermion charge, G_F the Fermi constant, and D=1 for leptons, 3 for quarks.

To good approximation, this cross section falls like s^{-1} which implies that as s increases we need corresponding large machine luminosities. The appropriate threshold factor which moderates this cross section is $\beta_f(3-\beta_f^2)/2$, where β_f is the fermion velocity.

This covers the production mechanism for h, ℓ and $L^\pm$. They will decay via the standard Weak Interaction, namely

$$h \longrightarrow \ell\, W^+ \quad \llcorner\!\!\longrightarrow f\bar{f}$$

$$\ell \longrightarrow t\, W^- \quad \llcorner\!\!\longrightarrow f\bar{f}$$

$$L^{\pm} \longrightarrow \nu_L\, W^{\pm} \quad \llcorner\!\!\longrightarrow f\bar{f}$$

where $f(\bar{f})$ are now 1st, 2nd and 3rd generation fermions. Depending on the mass differences involved, the W can be either real or virtual. For all the studies presented here, we take the top quark mass to be 40 GeV/c^2. None of the conclusions changes dramatically if M_t is in fact heavier.

What are the background processes which could inhibit the search for 4th generation fermions? There are three obvious sources of background:

1. Conventional processes from the three light generations. This background will prove to be large for searches done using $R = \sigma_{had}/\sigma_{\mu\mu}$, while $e^+e^- \rightarrow t\bar{t}$ will be a contributing background in topological searches.

2. Two-photon production of hadrons. This process has a very large cross section. However, if the hadronic system carries sufficient energy to be a serious background, the effective cross section becomes small enough to ignore. This is shown in Fig. 1 where the two-photon cross section is a function of $\sqrt{s}$. In this figure, the fraction of energy carried by the hadronic system is denoted by f.

3. We encounter a background at these energies not yet seen in e^+e^- machines, namely $e^+e^- \rightarrow W^+W^-$. This is in fact the main background since it has a large cross section and can easily mimic the decays of the h, ℓ and $L^{\pm}$.

The W pair production occurs via the three Feynman graphs shown in Fig. 2, and will be studied at LEP200. We have assumed here the Standard Model for

calculating cross sections and kinematic distributions. $\sigma_{W^+W^-}$ grows rapidly with $\sqrt{s}$, mainly due to the t channel ν exchange graph in Fig. 2. This growth, however, is mostly in the forward direction (see Fig. 3), so this background can be reduced by requiring that the event thrust axis not point in the forward direction.

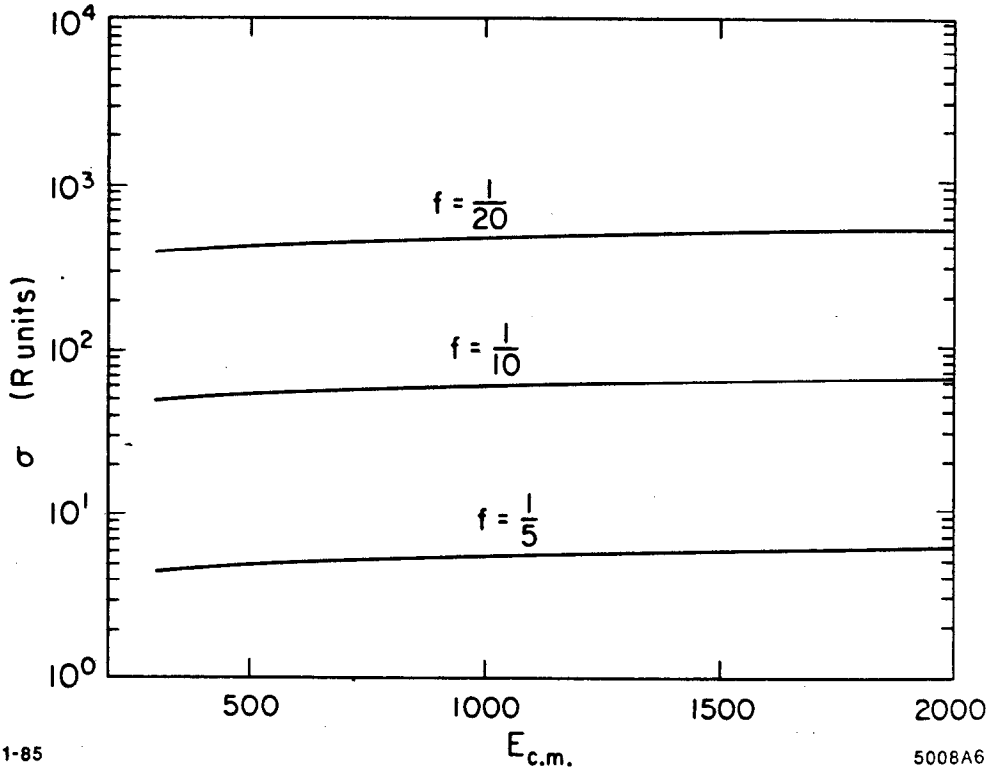

Fig. 1. R for e^+e^- + hadrons via the two-photon process. f is the fraction of energy carried by the hadronic system.

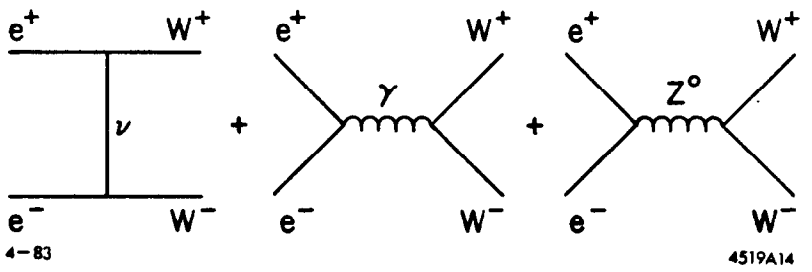

Fig. 2. Feynman graphs for the process $e^+e^- \rightarrow W^+W^-$.

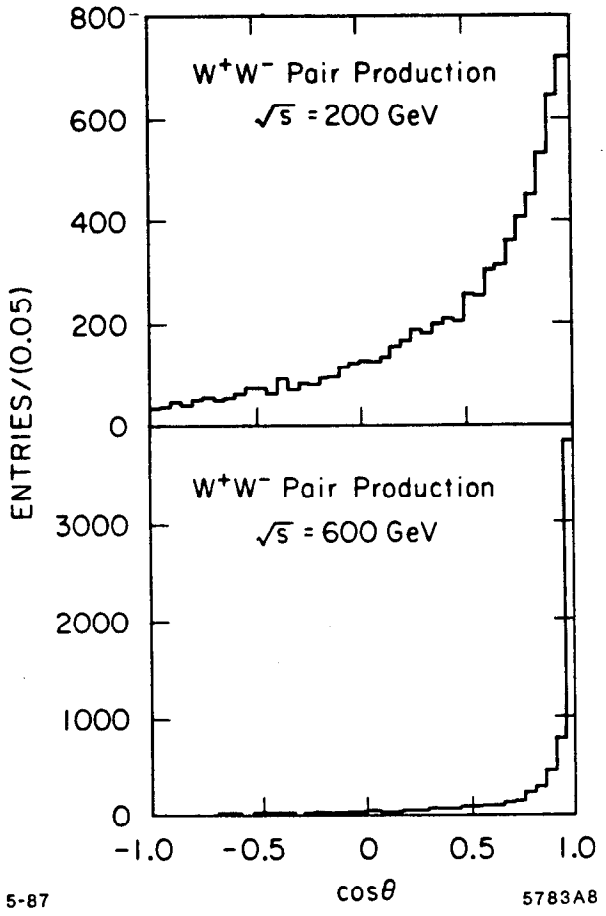

Fig. 3. Angular distribution of W^+ with respect to the e^- beam direction at $\sqrt{s} = 200$ GeV and $\sqrt{s} = 600$ GeV.

The cross section for the production of the 4th family fermions and the two major backgrounds are shown in Figs. 4 and 5. These cross sections have been corrected for initial state electromagnetic radiative effects, which is a particularly large, positive correction for the conventional light quarks. This comes about when the radiation is sufficiently large to generate the e^+e^- collision at M_Z, where the cross section is enormous. As we will see, these events are easily removed with simple kinematic cuts. Figures 4 and 5 set the magnitude of the rejection required to extract the 4th family signals.

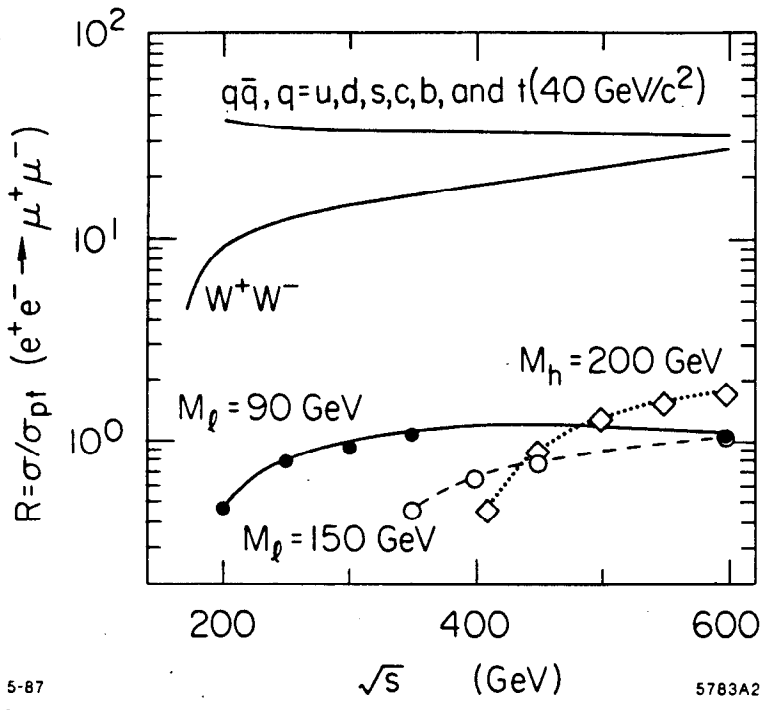

Fig. 4. Radiatively corrected R values of 4th family quarks and the two major backgrounds.

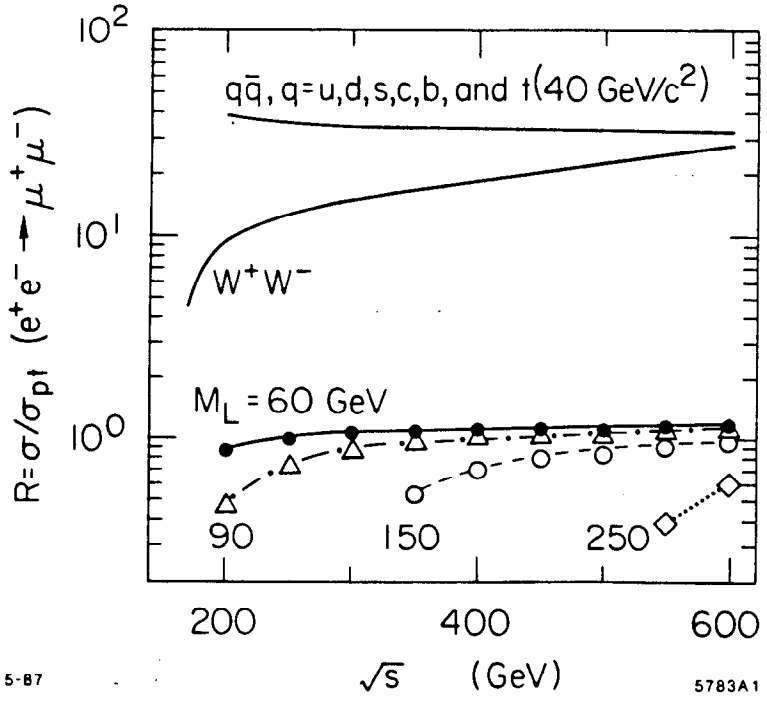

Fig. 5. Radiatively corrected R values of 4th family charged leptons and the two major backgrounds.

3. Establishing the Existence of h, ℓ or $L^{\pm}$

The first thing that comes to mind at a new e^+e^- collider is to look for an increase in R. By looking at Figs. 4 and 5 it becomes clear that even if one were above threshold, the increase in R from 4th family charged fermions is at most 3%. Since the PEP and PETRA experiments achieve systematic errors no better than 3% for R measurements, this procedure will not work.

It proves much more fruitful to look for distinctive topologies. By making relatively simple kinematic cuts one could greatly reduce the contribution to R from the light quarks and the W^+W^- backgrounds. Under these circumstances one could probably turn this into a useful search procedure. By adding the additional requirement of an isolated lepton, signal to background improves even more. Since leptonic decays are reasonably copious, this is not a large price to pay.

For all the charged fermion searches discussed here, Monte Carlo simulations were done for both the signal and background channels. In all cases, the Standard Model was assumed and initial state radiative processes were included. High-energy linear colliders will not have the well-defined $\sqrt{s}$ which e^+e^- storage rings provide. The machine parameters chosen to achieve high luminosity result in large ($\simeq$30%) uncertainties in the beam energy because of the intense radiation emitted when the beams pass through each other (beamstrahlung). Hence, at energies above LEP200 we have to avoid analysis techniques which rely on a precise knowledge of $\sqrt{s}$. These beamstrahlung effects have not been included in the heavy quark searches considered here because the search technique uses kinematic selection cuts which are relatively immune to the beam spread. However, this is more crucial for the $L^{\pm}$ search and in this case we have included the beamstrahlung effects.

3.1 SEARCH FOR THE 4TH GENERATION QUARKS $h(2/3)$, $\ell(-1/3)$

These searches rely heavily on the fact that the decays of the h and ℓ produce isolated leptons with very large transverse momentum. In addition, their kinematics differ considerably from the background processes, particularly at the higher energies. The signal topologies are shown in Figs. 6(a) and 6(b) and are characterized by isolated leptons and high aplanarity. (Aplanarity is a measure of the amount of momentum which is perpendicular to the event plane as defined by a sphericity analysis.) The background topologies shown in Fig. 7 are characterized by relatively low multiplicity and aplanarity and mostly lower transverse momentum for the e and μ. Based on the actual kinematic distributions, the following set of cuts were used:

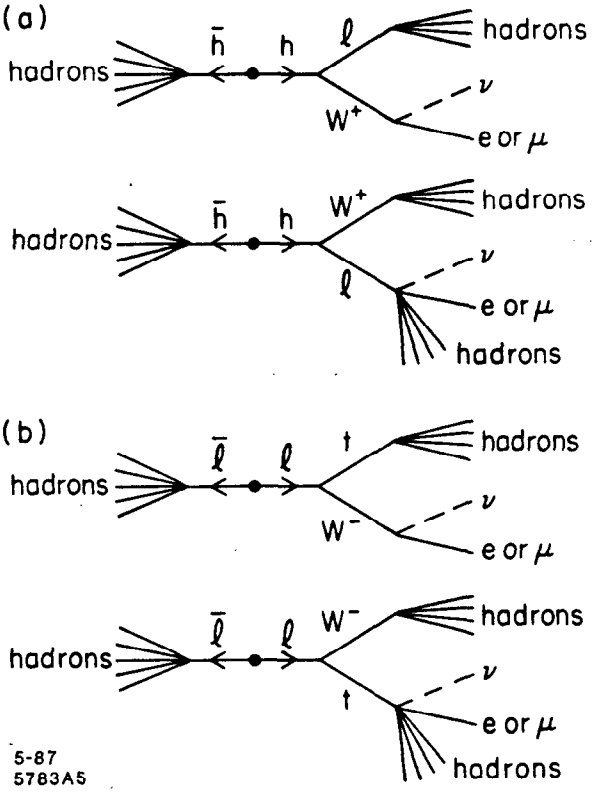

Fig. 6. Signal topologies used to search for h and ℓ.

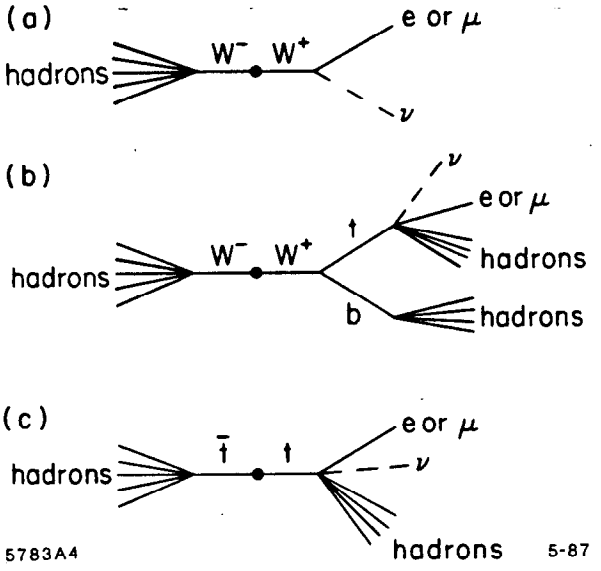

Fig. 7. Background sources for the search for h and ℓ.

(a) Aplanarity > 0.2; $\sqrt{s} = 200$ GeV, > 0.15, $\sqrt{s} = 600$ GeV.

(b) Charged particle multiplicity > 35.

(c) Isolated lepton; < 100 MeV of energy within a 10° cone centered around the lepton direction.

The means of the distributions for (a) and (b) are given in Table I for the signal and background channels. The parameters for the simulations were:

$$\sqrt{s} = 200 \text{ GeV}; \quad M_\ell = 90 \text{ GeV/c}^2 \quad \text{(no } h \text{ is reasonable)}$$

$$< \mathcal{L} > = \frac{1}{2} \times 10^{32} \text{ cm}^{-2} \text{ sec}^{-1} .$$

$$\sqrt{s} = 600 \text{ GeV}; \quad M_\ell = 150 \text{ GeV/c}^2 \quad M_h = 200 \text{ GeV/c}^2$$

$$< \mathcal{L} > = \frac{1}{2} \times 10^{33} \text{ cm}^{-2} \text{ sec}^{-1} .$$

The results of this study are summarized in Tables II and III where we have assumed a six-month run. The apparently high efficiency for isolated lepton events in the signal channels occurs because in many events more than one lepton

is detected. The background from misidentifying hadrons as leptons has been included assuming the misidentification probability of $\frac{1}{2}\%$. This is modest, since these leptons are truly isolated, and most detectors will do much better. The lepton transverse momentum spectra are shown in Figs. 8 and 9. One concludes from this study that both at $\sqrt{s}$= 200 GeV and at higher energies ($\sqrt{s}$= 600 GeV being typical) one has a relatively clean signal for h and ℓ and that the efficiencies of such searches are large enough to yield sizeable signals in a period of six months or less.

Table I.

Channel	<Aplanarity>	<Charged Multiplicity>
$\sqrt{s}$ = 600 GeV		
$h\bar{h}$	.26	77.1
$\ell\bar{\ell}$	.20	62.2
W^+W^-	.08	31.2
light quarks	.07	29.7
$\sqrt{s}$ = 200 GeV		
$\ell\bar{\ell}$	.28	44.2
W^+W^-	.19	29.8

Table II. $\sqrt{s}$ = 600 GeV

Channel	# Produced	# Isolated Leptons
$h\bar{h}$	3,000	2873
$\ell\bar{\ell}$	2,060	1017
W^+W^-	37,500	212
light quarks	60,000	147
Misidentification of hadrons	97,500	60

Table III. $\sqrt{s} = 200$ GeV

Channel	# Produced	# Isolated Leptons
$\ell\bar{\ell}$	825	495
W^+W^-	14,850	685
light quarks	63,000	124

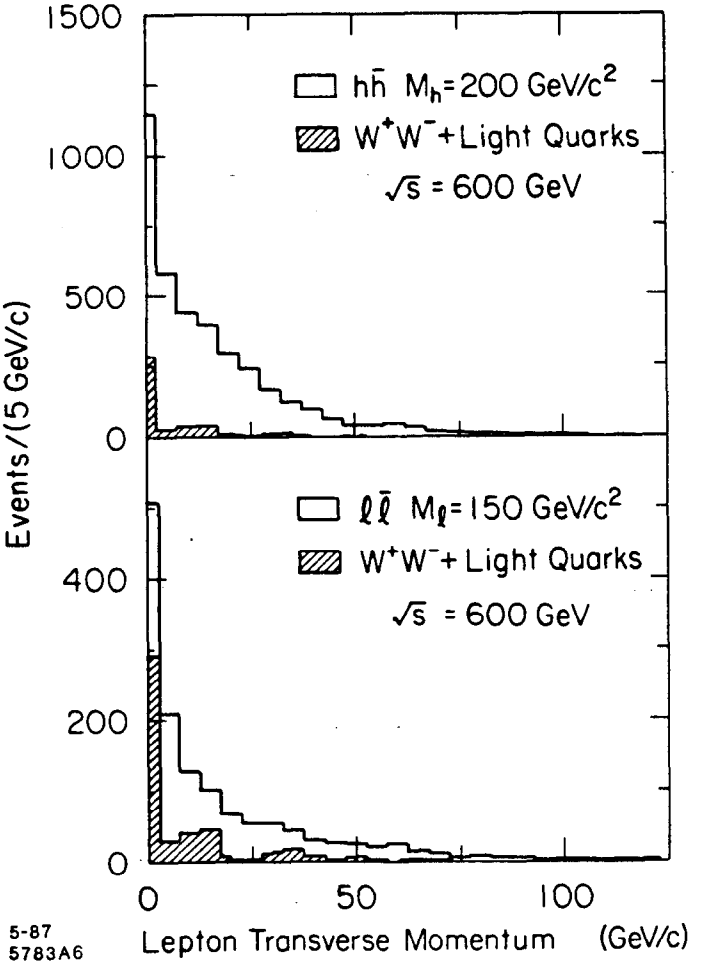

Fig. 8. Lepton transverse momentum for the events selected for the h and ℓ search and for the contributions from the background ($\sqrt{s} = 600$ GeV).

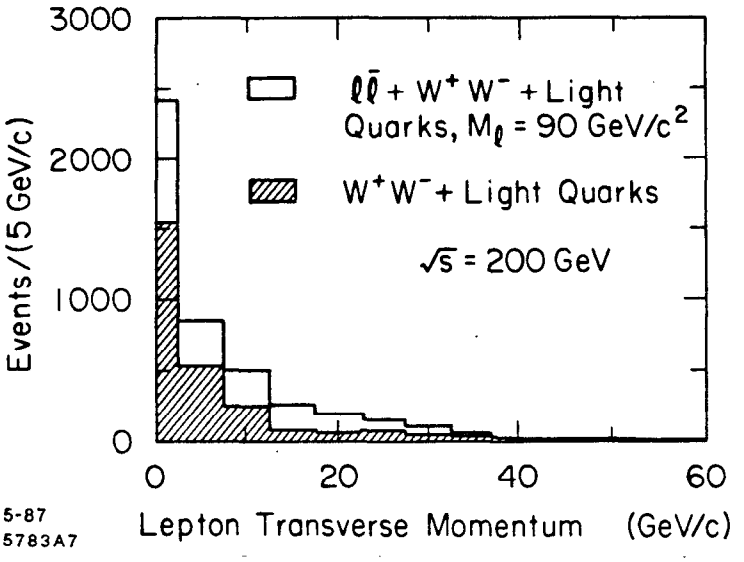

Fig. 9. Lepton transverse momentum for the events passing the selection criteria at $\sqrt{s} = 200$ GeV. The shaded region shows the contributions from the background; the unshaded, the contribution from the signal plus background.

3.2 Search for the 4th Generation $L^{\pm}$

Figure 10(a) shows the signal topology used for the $L^{\pm}$ search, while Fig. 10(b) shows the main background topology. In order to generate a clean signature, we have concentrated here on the leptonic decay of the $L^{\pm}$, where one pays a fairly large price in terms of their branching fraction [$B(L^{\pm} \rightarrow e\nu_e\nu_L) \approx 8\%$]. The alternative would be to use the hadronic decays of the $L^{\pm}$ which have larger branching fractions. This will probably work, but has not been tried here. The characteristics which let one separate the signal and background topologies are: 1) the fact that the background tends to be peaked in the forward direction, 2) there is small missing energy on the hadronic side of the event and 3) there is an isolated lepton on the other side of the event which is accompanied by large missing transverse momentum which is carried off by ν_L. For LEP200 the beam energy will be accurately known and this can be used to take maximum advantage of these characteristics. However, for the 600 GeV linear collider where the beam energy is poorly known, a less optimal set of cuts are possible.

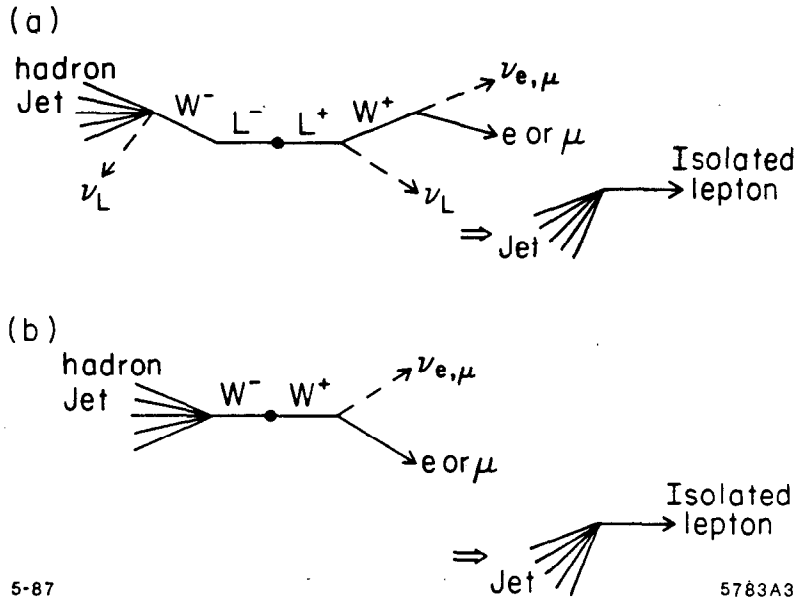

Fig. 10. (a) Signal topology selected for $L^{\pm}$ search and (b) Major background topology (W^+W^-).

3.2.1. Analysis at $\sqrt{s} = 200$ GeV

Cuts can be made which take advantage of the above characteristics of signal and background. In addition, if one *assumes* a W^+W^- hypothesis, $\overline{P}_{\nu_\ell}$ can be reconstructed. In the W^+W^- case, the invariant mass ($M_{\nu_\ell \ell}$) of this ν_ℓ and the isolated lepton shows a distinct mass peak. The extra neutrinos in the L^+L^- topology makes the assumption of W^+W^- kinematics incorrect, $\overline{P}_{\nu_\ell}$ is reconstructed incorrectly, and $M_{\nu_\ell \ell}$ does not show any peaks as shown in Fig. 11. Therefore, the following set of cuts were used:

(a) $|\cos\theta_{\rm thrust}| < 0.85$; thrust is that of the hadronic jet.

(b) Isolated $e^{\pm}$ or $\mu^{\pm}$. Require < 1 GeV within a 30° cone around the lepton.

(c) $E_{\rm vis}$ = measured energy in hadronic hemisphere,

$$E_{vis} < 0.8\ E_{beam} \quad .$$

(d) Assume W^+W^- event. Reconstruct $\overline{P}_{\nu_\ell}$ and calculate $M_{\nu_\ell \ell}$. Demand $M_{\nu_\ell \ell} < 78$ GeV; $M_{\nu_\ell \ell} > 86$ GeV (not near M_W).

Using a luminosity of $< \mathcal{L} >= \frac{1}{2} \times 10^{32}$ cm^{-2} sec^{-1} over a six-month run, a lepton mass of $M_{L^\pm} = 90$ GeV, and a massless ν_L, results of this study are summarized in Table IV.

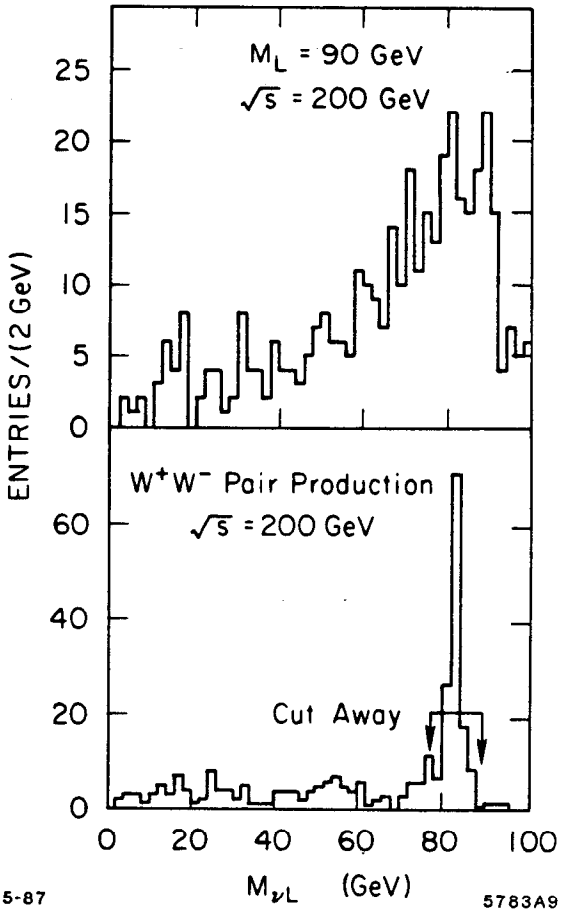

Fig. 11. After *assuming* a W^+W^- event and reconstructing $\overline{P}_{\nu_\ell}$, the invariant mass of the isolated lepton and ν^ℓ. Top: L^+L^- events. Bottom: W^+W^- events.

Table IV. $\sqrt{s} = 200$ GeV, $M_{L^\pm} = 90$ GeV

Channel	# Produced	# Passing Cuts
L^+L^-	1,100	39
W^+W^-	14,850	10
light quarks	63,000	3

3.2.2 Analysis of $\sqrt{s} = 600$ GeV

The analysis techniques for $\sqrt{s}$ of 200 GeV and 600 GeV differ because the higher luminosity required for the 600 GeV machine will result in synchrotron radiation in the collision region (beamstrahlung) which leads to substantial smearing of the center-of-mass energy of annihilation. Therefore, we will not know $\sqrt{s}$ (or E_{beam}) with any degree of precision, and should develop techniques which do not rely on these parameters and which are not sensitive to arbitrary boosts along the axis of the beam (z-axis).

Looking in the transverse plane of the event, a W^+W^- hypothesis is again assumed as shown in Fig. 12. The invariant mass of the leptonic decay is insensitive to boosts along the z-axis, and we have:

$$M_W^2 = (E_\ell + E_\nu)^2 - (P_{\ell x} + P_{\nu x})^2 - (P_{\ell y} + P_{\nu y})^2 - (P_{\ell z} + P_{\nu z})^2 \quad .$$

Using this equation, and knowing that the transverse momentum of the hadronic side must be balanced by transverse momentum on the leptonic side, a quadratic equation in $P_{\nu z}$ is derived. In the case of L^+L^-, the assumption of W^+W^- kinematics is incorrect, and quite often imaginary solutions for $P_{\nu z}$ are obtained. Cuts can then be made on η, the discriminant of the solution to the quadratic, where $\eta < 0$ indicates imaginary solutions.

Event samples were generated by Monte Carlo from distributions of electron and positron energies computed using a beam-beam simulation code written by

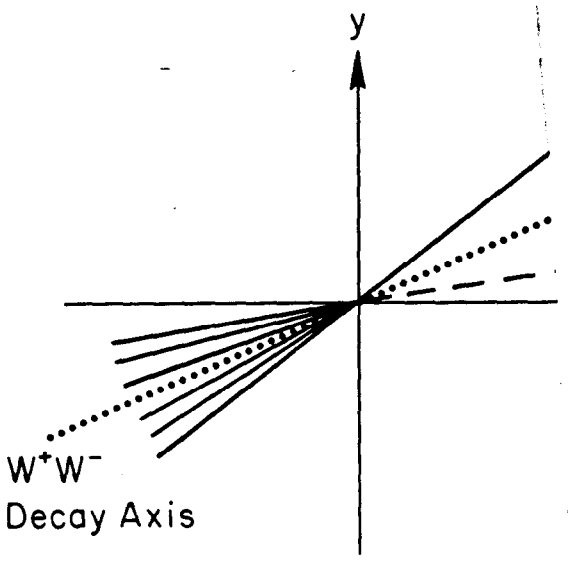

Fig. 12. Transverse plane of W^+W^- background event. P_x, P_y of the hadronic jet hemisphere must be balanced by the lepton hemisphere.

K. Yokoya[1] based on typical sets of machine parameters for a 600 GeV collider. Cuts used were:

(a) $|\cos\theta_{\text{thrust}}| < 0.6$; thrust is that of the hadronic jet.

(b) Isolated $e^{\pm}$ or $\mu^{\pm}$ with same requirements as $\sqrt{s} = 200$ GeV case.

(c) η = discriminant of solution to quadratic in $P_{\nu z}$,

$$\frac{\eta}{M_W^6} < 0.1 \quad .$$

Using $< \mathcal{L} >= \frac{1}{2} \times 10^{33}$ cm^{-2} sec^{-1} over a six-month run the results of this study for M_L= 150 and 250 GeV with $M_{\nu_L} = 0$ are summarized in Table V.

One concludes that at $\sqrt{s} = 200$ GeV, one has a relatively clear signal with high enough yield in a six-month run. At $\sqrt{s} = 600$ GeV, the signal is less clear because of problems caused by beamstrahlung, but is still evident. In both cases, after cuts are made, the momentum spectrum of the isolated lepton can be examined. The two-body decay of the $W^{\pm}$ results in a lepton momentum

Table V. $\sqrt{s} = 600$ GeV

Channel	# Produced	# Passing Cuts
L^+L^-		
M_L= 150 GeV	1,860	74
M_L= 250 GeV	1,200	69
W^+W^-	37,500	54
Light quarks	60,000	6

spectrum peaked at high momentum, whereas the lepton from $L^{\pm}$ decays has a much softer momentum spectrum. Fits can then be made to determine the presence of a L^+L^- signal.

4. Searching for Neutral Heavy Leptons

We consider now the possibility that the 4th family comprises $L^{\pm}$, L° where L° is a massive Dirac neutrino.

The production is via $e^+e^- \rightarrow L^{\circ}\bar{L}^{\circ}$ with a cross section given by

$$\frac{d\sigma}{d\cos\theta} = \frac{1}{64\pi} \frac{G_F^2 s}{((1 - s/M_z^2)^2 + M_z^2/M_z^2)} \{(1 - 4\sin^2\theta_w + 8\sin^4\theta_w)$$

$$+ \beta(1 + \beta^2 cos^2\theta) + 2(1 - 4sin^2\theta_w)\beta^2 cos\theta\}$$

where β is the L° velocity and θ_w is the weak mixing angle. For $s \ll M_Z^2$:

$$\sigma \sim \frac{0.025}{s(\text{TeV})} \text{ pb} .$$

This gives $\sigma = 1$ pb ($R = 0.43$) at $\sqrt{s} = 200$ GeV and $\sigma = 0.07$ ($R = 0.27$) for $\sqrt{s}$ = 600 GeV. Hence, there is substantial production of $L^{\circ}\bar{L}^{\circ}$. There are several modes for decay, examples of which are given below.

Within the Standard Model one can have:

1. $L^\circ \to L^- W^+ \qquad (M_{L^\circ} > M_{L^-})$
2. Mixing with a lighter generation (presumably the τ, but e and μ are not excluded):

$$L^\circ \to \tau^- W^+ \ .$$

For a mixing angle ϵ, the weak iso-doublets are

$$\begin{pmatrix} \nu_\tau \cos\epsilon + L^\circ \sin\epsilon \\ \tau^- \end{pmatrix}_L \quad \begin{pmatrix} L^\circ \cos\epsilon - \nu_\tau \sin\epsilon \\ L^- \end{pmatrix}_L .$$

3. One can also imagine decays which violate the Standard Model like the flavor-changing neutral current decay where the L° mixes with ν_τ:

$$L^\circ \to Z^\circ \nu_\tau \ .$$

All of these decay scenarios lead to striking signatures with no obvious backgrounds. The distinctive features are low multiplicity and multiple, mixed leptons. For illustrative purposes we choose Model 2 in which the L° couples to the τ. We can define two classes of search topologies:

1. Four-charged particle events in which both the τ and intermediate W decay leptonically. Using standard branching fractions, this topology occurs in 2% of the $L^\circ \bar{L}^\circ$ events and results in events of the type $\ell\ell\ell\ell$, $\ell\ell\pi\pi$, $\ell\ell\ell\pi$ (where $\ell = e$ or μ) with a ratio of $e : \mu$: π of 1:1:2.5. We label these $2+2$ events.
2. Events with two-charged particles in one hemisphere and a high-multiplicity jet in the other hemisphere. Again the low-multiplicity hemisphere is populated with mixtures of e, μ and π. This process occurs in 20% of the $L^\circ \bar{L}^\circ$ events and we label it the $2+N$ topology.

If we assume as before $< \mathcal{L} >= \frac{1}{2} \times 10^{32}$ cm^{-2} sec^{-1} at $\sqrt{s} = 200$ GeV, $< \mathcal{L} >= \frac{1}{2} \times 10^{33}$ cm^{-2} sec^{-1} at $\sqrt{s} = 600$ GeV and a six-month run, one finds the number of events shown in Table VI for the $2 + 2$ topology and the $2 + N$ topology. This would be sufficient to establish the signal, since there appear to be no competing backgrounds.

Table VI.

Topology	# Events 600 GeV	# Events 200 GeV
$2 + 2$	9	14
$2 + N$	100	160

5. Conclusions

We have studied the possibilities for the discovery of 4th family fermions in e^+e^- machines at energies beyond the Z°. Two specific energies were chosen: $\sqrt{s} = 200$ GeV, compatible with the highest LEP200 energy and $\sqrt{s} = 600$ GeV, which serves as a reasonable example for machines in the 500–1000 GeV region. These Monte Carlo studies are by no means exhaustive, nor have they included the effects of detector inefficiencies and resolutions. However, it appears that sufficiently clean topologies exist for the discovery of all the 4th family charged fermions and the neutral if it is a massive Dirac particle. Production cross sections and topological search efficiencies are sufficiently large that with the LEP200 design luminosity or a 10^{33} cm^{-2} sec^{-1} luminosity at $\sqrt{s} = 600$ GeV, sizeable signals are obtained in six-month running periods. In short, the outlook for the discovery of 4th family fermions in these higher energy e^+e^- machines looks very promising. More detailed studies,[2] including the effects of detector smearing and acceptance, are underway at SLAC for $\sqrt{s} = 600$–1000 GeV. A report on this work should be forthcoming soon.

Acknowledgments

The authors wish to thank Alfred Peterson for providing the Monte Carlo implementation and tapes for this study. Useful discussions with Gary Feldman are also acknowledged.

References

1. K. Yokoya, SLAC–AAS–27 (1987).
2. These have been performed by members of the e^+e^- Study Group at Stanford Linear Accelerator Center, Chaired by Michael Peskin.